

MACHINE LEARNING ASSISTED BAYESIAN CALIBRATION OF ACCELERATOR DIGITAL TWIN FROM ORBIT RESPONSE DATA*

W. Lin^{1,†}, K. A. Brown¹, G. H. Hoffstaetter de Torquat^{1,2}, C. Kelly³, N. Urban⁴

¹Collider-Accelerator Department, Brookhaven National Laboratory, Upton, NY, USA

²CLASSE, Cornell University, Ithaca, NY, USA

³Computational Science Department, Brookhaven National Laboratory, Upton, NY, USA

⁴Applied Mathematics Department, Brookhaven National Laboratory, Upton, NY, USA

Abstract

Digital twins of particle accelerators are used to plan and control operations and to design data collection campaigns. Accurate modeling typically requires knowledge of quantities that are hard to measure directly, e.g., magnet alignments, power supply transfer functions, magnet nonlinearities, and stray fields. In this work we introduce multiplicative nuisance parameters to the quadrupole transfer functions to parametrize these effects and use Bayesian methods to probabilistically estimate their values and uncertainties by calibrating the Bmad digital twin to beam measurements performed at the AGS Booster at Brookhaven National Laboratory. The inference is computationally accelerated using a machine learning emulator of the physical accelerator digital twin trained to a perturbed-parameter ensemble of Bmad simulations. The result is a joint posterior distribution over the nuisance parameters constrained by the data and taking into account beam monitor errors. Incorporating estimates of the nuisance parameters into the digital twin is shown to result in a significant improvement in the quality of the model and provides error bars on the model parameters and predictions.

INTRODUCTION

The Alternating Gradient Synchrotron (AGS) Booster acts as the pre-injector for the AGS, increasing the AGS injection energy from 200 MeV to 1.5 GeV [1]. It also serves as a heavy-ion source for the NASA Space Radiation Laboratory. As one of the most upstream components in the acceleration chain, accurate control of beam properties in the Booster is indispensable to providing high quality beams to both the Relativistic Heavy Ion Collider (RHIC) and the future Electron Ion Collider (EIC).

A good understanding of magnet properties in the Booster is essential for better beam control. A comparison of measured and simulated orbit response data reveals that the current Booster digital twin is inaccurate at the level of several percent. The overarching goal of our research is to utilize Bayesian uncertainty quantification (UQ) techniques to identify and model the sources of these discrepancies.

As a first step in this direction, we focus on the uncertainties associated with the 48 quadrupole magnets, as these

are expected to play a dominant role. We introduce magnet-dependent nuisance parameters to the transfer function that relates the magnetic field to the power supply current, allowing the unknown sources of error to individually affect the magnet's impact on the beam orbit.

The values of these nuisance parameters are constrained using experimental data via Bayesian UQ. The resulting posterior distribution provides data-constrained values for the nuisance parameters that are then incorporated into the digital twin to improve the modeling.

ORBIT RESPONSE MEASUREMENT

To collect suitable data from the Booster we developed a script [2] that sets each corrector in turn to three settings: zero kick (baseline value), positive kick, and negative kick, while leaving all other correctors in their baseline setting. After setting the corrector, live beam position monitor (BPM) data and all the magnet settings are saved. The script work flow is outlined in Fig. 1.

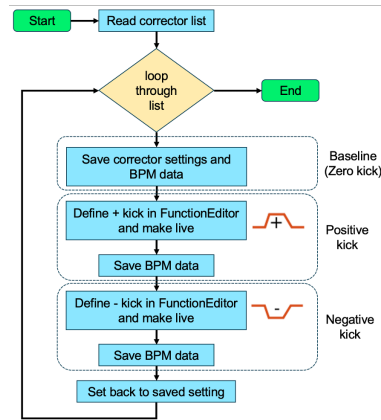


Figure 1: Work flow of orbit response measurement script.

The script was applied to both the 24 horizontal and 24 vertical correctors in the Booster. Each corrector was set to $\pm 22\text{ A}$ between 50 and 110 milliseconds during the Booster magnet cycle. In this work we utilize only the data collected at a flat-top time of 92 ms. For each setting, between 2 and 5 (typically 3) repeated measurements were taken over different cycles, for a total of 224 and 113 measurements for the horizontal and vertical correctors, respectively.

The data collected comprises both orbit data and all magnet current settings in the Booster, including dipoles, quadrupoles, sextupoles, and all correctors. These settings

* Work supported by Brookhaven Science Associates, LLC under Contract No. DE-SC0012704 with the U.S. Department of Energy and by DOE-NP No. DE SC-0024287.

† wlin1@bnl.gov

can be input to the physics simulation model, constructed in Bmad [3], to produce simulated orbit data.

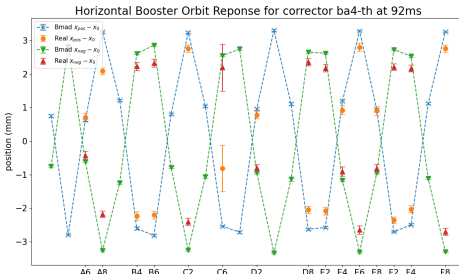


Figure 2: Comparison between measured and simulated vertical orbit responses with corrector ba4-th set to ± 22 A, data taken at 92 ms in the Booster cycle. The larger error on BPM C6 is due to a known hardware problem.

A comparison of the orbit differences between positive, zero, and negative corrector settings for one corrector (ba4-th) is shown in Fig. 2. The error bars are estimated based on the fluctuations over the repeated measurements. We observe that the difference between measured and simulated differential orbits are mostly within 1 mm, but still much larger than the error bars of the measurements. This discrepancy implies there are sources of error in the real machine that are not included in the simulation model.

BOOSTER QUADRUPOLE TRANSFER FUNCTION

There are 48 quadrupoles (24 in each plane) in the Booster, powered in series with the main bending dipoles. The simulation employs a fifth order polynomial to model the gradient of a quadrupole's magnetic field as a function of its power supply current, I_q :

$$\frac{\partial B}{\partial r} = a_0 + a_1 \cdot I_q + a_2 \cdot I_q^2 + a_3 \cdot I_q^3 + a_4 \cdot I_q^4 + a_5 \cdot I_q^5 \quad (1)$$

where r is the radial distance. The normalized gradient k_1 equations we need to consider are:

$$k_{1,H} = \frac{1}{B\rho L} \left\langle \frac{\partial B}{\partial x} \right\rangle, \quad k_{1,V} = \frac{1.003}{B\rho L} \left\langle \frac{\partial B}{\partial y} \right\rangle \quad (2)$$

where $\frac{\partial B}{\partial x}$ and $\frac{\partial B}{\partial y}$ are obtained via Eq. 1. The polynomial coefficients are derived from a least-squares linear regression fitting to match the tune measurement data from 1992 and 1993 [4].

All quadrupoles receive the same current due to being wired in series, and the currents remain fixed in our data up to small power supply fluctuations. As such, the transfer function can be treated essentially as a magnet-independent constant. This provides a convenient location to introduce magnet-dependent properties that parametrize the model uncertainties. Specifically, we allow for magnet-dependent perturbations in the field strength through multiplicative nuisance parameters $var^{(x)}$ and $var^{(y)}$ for the x - and y -plane quadrupoles, respectively. The resulting k_1 of the quadrupoles in the model are therefore defined as:

$$(k'_{1,H})_i = var_i^{(x)} k_{1,H}, \quad (k'_{1,V})_i = var_i^{(y)} k_{1,H} \quad (3)$$

where $i \in \{1 \dots 24\}$ indexes the quadrupole magnet.

BAYESIAN UNCERTAINTY QUANTIFICATION

Uncertainty quantification is the process of identifying and quantifying uncertainties in models and simulations with the goal of exploring how uncertainties in model parameters or assumptions affect the outputs. A common method for UQ is Bayesian inference, which seeks to constrain or probabilistically “fit” model parameters using measurement data. Bayesian UQ takes expert knowledge of the model parameters θ as priors $p(\theta)$ as well as a probability model of the data-generating process $p(x|\theta)$ called the likelihood function. By constraining the parameters with data samples $\mathcal{D}_n = \{x_1, \dots, x_n\}$, Bayesian UQ updates the model and calculates the posterior probability distribution $p(\theta|\mathcal{D}_n)$ of parameters θ given the data \mathcal{D}_n . According to Bayes’ Theorem, the posterior distribution is given by [5]:

$$P(\theta|x_1, \dots, x_n) = \frac{p(\mathcal{D}_n|\theta)p(\theta)}{p(\mathcal{D}_n)} = \frac{\mathcal{L}_n(\theta)p(\theta)}{c_n} \quad (4)$$

If the data points $\mathcal{D}_n = \{x_1, \dots, x_n\}$ are statistically independent, then the likelihood function $\mathcal{L}_n(\theta) = \prod_{i=1}^n p(x_i|\theta)$ factorizes into the product of likelihoods of each individual data point. The denominator of Eq. (4), $c_n = \int \mathcal{L}_n(\theta)p(\theta) d\theta$, is referred to as the evidence and usually does not need to be calculated when using Monte Carlo sampling, as we will use here. In summary, the posterior is proportional to the product of the likelihood and the prior:

$$p(\theta|\mathcal{D}_n) \propto \mathcal{L}(\theta)p(\theta) \quad (5)$$

The likelihood function is given by the probability model $x = m(\theta; I_q) + \epsilon$ where $m(\cdot; \cdot)$ is the prediction of (a machine learning emulator of) the Bmad model as a function of its uncertain parameters θ and known input currents I_q , and ϵ is an independent and identically distributed (*iid*) normal random error variable.

In our case, priors are required for the 24×2 nuisance parameters (henceforth, “vars”). We employ lognormal priors, a conventional choice for multiplicative parameters that ensures an unbiased distribution for the resulting transfer function, and adjust the parameters such that the mean is fixed to unity and the variance to some chosen value.

The likelihood function computes the expected orbit given specific values of the vars and of the “controls”: the settings for the correctors and the associated dipole and vertical and horizontal quadrupole and sextupole currents. During inference, these control settings (baseline, positive, and negative) are taken from the stored data files.

To map the controls to the orbit we employ a surrogate model of the Bmad simulator (see below), which provides expected beam positions as a function of the controls and vars. To model the aleatoric errors in the BPMs we use the simulated values as the means of a normal distribution with a variance of $\epsilon = \sqrt{2}\sigma_{\text{BPM}}$ where $\sigma_{\text{BPM}} = 0.15$ mm is the expected BPM error and the $\sqrt{2}$ is required due to the output being an orbit difference.

We perform the inference using the Julia “Turing” package [6] to sample the posterior distribution.

SURROGATE MODEL

Efficient sampling of the high-dimension posterior distribution is achieved using the “No U-turn Sampler”, a variant of “Hamiltonian Monte Carlo” Markov chain algorithm [7]. This algorithm requires accurate evaluation of the derivatives of the simulated result, something that Bmad is presently unable to provide. A fast simulation is also important as the sampling can require many thousands of evaluations. These requirements spurred the introduction of a machine-learning surrogate model for the Bmad simulation.

We employ a ResNet-style architecture [8] with ~ 360 k parameters, comprising 77 input and 15-18 output features with two hidden fully-connected layers of dimension 400×400 , each sandwiched within a skip connection, which allows each layer to model the residuals of the previous layers and stabilizes the model against vanishing parameter gradients. Separate models were trained for the x - and y -plane orbits, each based on 820-890k simulated sample data points.

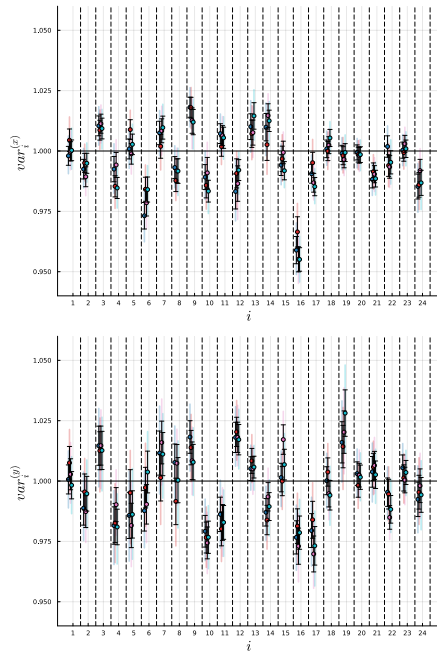


Figure 3: The inferred x - (upper) and y -plane vars for each of the 24 associated quadrupoles. For each magnet i we plot left-to-right values obtained from different datasets of orbit response data. The darker and lighter error bars indicate the 68 % and 95 % confidence bands, respectively.

UQ RESULTS ON BOOSTER ORM

Given the available data, there are many possible orbit responses that can be incorporated into the inference. Of those examined, we found that responses between -22 A and $+22$ A for each varied corrector led to the smallest uncertainty on the vars, likely because these large before and after current settings amplify the digital twin errors.

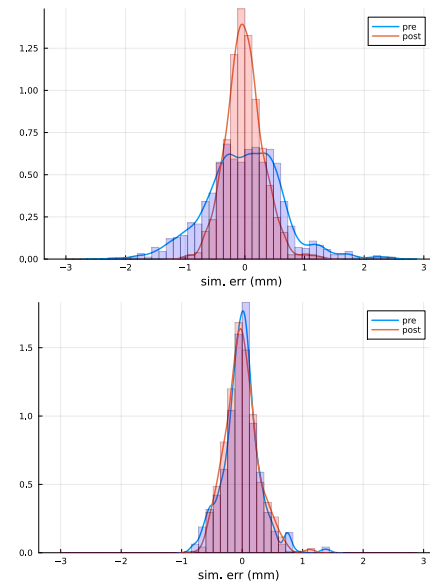


Figure 4: Simulation error in x - (upper) and y -plane (lower) compared to measurements with (red) and without (blue) posterior estimates of the quadrupole variations.

We constructed four such datasets in order to study the stability of the inference predictions. In Fig. 3 we show that the resulting inferred values are consistent across these different datasets, demonstrating the stability of our results. The majority of the inferred vars are consistent with unity but there are several that are significantly different from one, notably x -quad 16. The resulting posterior samples for these four data sets were combined (pooled) to obtain our best estimates of the vars.

Figure 4 shows the result of taking the central value (point estimates) of our results and incorporating these into the Bmad digital twin. We observe that UQ was able to identify errors that effectively decrease the simulation errors, especially in the horizontal plane.

CONCLUSION

In this work, we employed Bayesian uncertainty quantification to identify the effect of errors in simulating the quadrupole magnets on the Booster orbit response. We demonstrate that incorporating the resulting error estimates can significantly improve the agreement between simulation model and real measurements, making UQ a powerful tool for accelerator digital twin development.

REFERENCES

- [1] M. Shieh, AGS booster celebrates a quarter-century of service. <https://www.bnl.gov/newsroom/news.php?a=26425>
- [2] L. Hajdu, V. Schoefer, S. Nemesure, and J. Morris, Booster orbit corrector response measurement and introduction to CAD software tools, 2023. <https://docs.google.com/presentation/d/16zbquZRppY8-pajgdTJTM0F4MZ-1tKa5NIa6TNLRSc/edit?usp=sharing>
- [3] D. Sagan, “Bmad: a relativistic charged particle simulation library”, *Nucl. Instrum. Methods Phys. Res. A*, vol. 558, no. 1,

pp. 356–359, 2006. doi:10.1016/j.nima.2005.11.001

- [4] K. A. Brown, R. Fliller, W. Meng, and W. van Asselt, “A high precision model of AGS booster tune control”, in *Proc. EPAC'02*, Paris, France, Jun. 2002, paper THPLE112, pp. 548–550. <https://jacow.org/e02/papers/THPLE112.pdf>
- [5] L. Wasserman, “Bayesian inference”, in *All of Statistics: A Concise Course in Statistical Inference*. New York, NY: Springer New York, 2004, pp. 175–192.
doi:10.1007/978-0-387-21736-9_11
- [6] H. Ge, K. Xu, and Z. Ghahramani, “Turing: a language for flexible probabilistic inference”, in *Proceedings of the Twenty-*

First International Conference on Artificial Intelligence and Statistics, Playa Blanca, Lanzarote, Canary Islands, Spain, Apr. 2018, pp. 1682–1690. <https://proceedings.mlr.press/v84/ge18b.html>

- [7] M. D. Hoffman and A. Gelman, “The No-U-Turn sampler: adaptively setting path lengths in Hamiltonian Monte Carlo”, *arXiv*, 2011. doi:10.48550/arXiv.1111.4246
- [8] K. He, X. Zhang, S. Ren, and J. Sun, “Deep residual learning for image recognition”, *arXiv*, 2015.
doi:10.48550/arXiv.1512.03385